




ORIGINAL ARTICLE

Expanding the allelic spectrum of *ELOVL4*-related autosomal recessive neuro-ichthyosis

Fatima Alabdulrazzaq^{1,2}  | Talal Alanzi³ | Haya H. Al-Balool⁴ | Alice Gardham⁵  | Emma Wakeling⁶ | Harry G. Leitch^{5,7,8} | Moeenaldeen AlSayed^{9,10} | Maha Abdulrahim¹¹ | Abdulaziz Aladwani⁴ | Antonio Romito¹² | Kapil Kampe¹² | Sacha Ferdinandusse^{13,14} | Ashraf H. Aboelanine⁴ | Amira Abdullah¹ | Amal Alwadani⁴ | Laila Bastaki⁴ | Frédéric M. Vaz^{13,14}  | Aida M. Bertoli-Avella¹²  | Dana Marafi^{1,4,15} 

¹Department of Pediatrics, Adan Hospital, Ministry of Health, Hadiya, Kuwait

²Kuwait Institute of Medical Specialization, Sulaibkikhat, Kuwait

³Division Medical Genetics and Metabolic, Department of Pediatrics, Prince Sultan Military Medical City, Riyadh, Saudi Arabia

⁴Kuwait Medical Genetics Centre, Ministry of Health, Sulaibkikhat, Kuwait

⁵North West Thames Regional Genetics Service, Northwick Park Hospital, Harrow, UK

⁶North East Thames Regional Genetics Service, Great Ormond Street Hospital, London, UK

⁷Medical Research Council, London Institute of Medical Sciences, London, UK

⁸Institute of Clinical Sciences, Faculty of Medicine, Imperial College London, London, UK

⁹Department of Medical Genetics, King Faisal Specialist Hospital and Research Center, Riyadh, Saudi Arabia

¹⁰Faculty of Medicine, Alfaisal University, Riyadh, Saudi Arabia

¹¹King Abdullah Bin Abdulaziz University Hospital, Princess Nourah Bint Abdulrahman University, Riyadh, Saudi Arabia

¹²CENTOGENE GmbH, Rostock, Germany

¹³Amsterdam UMC Location University of Amsterdam, Department of Clinical Chemistry and Pediatrics, Laboratory Genetic Metabolic Diseases, Emma Children's Hospital, Amsterdam, The Netherlands

¹⁴Amsterdam Gastroenterology Endocrinology Metabolism, Inborn Errors of Metabolism, Amsterdam, The Netherlands

¹⁵Department of Pediatrics, Faculty of Medicine, Kuwait University, Safat, Kuwait

Correspondence

Dana Marafi, Department of Pediatrics, Faculty of Medicine, Kuwait University P.O. Box 24923, Safat 13110, Kuwait.
Email: dana.marafie@ku.edu.kw

Abstract

Background: Very long-chain fatty acids (VLCFAs) composed of more than 20 carbon atoms are essential in the biosynthesis of cell membranes in the brain, skin, and retina. VLCFAs are elongated beyond 28 carbon atoms by *ELOVL4* enzyme. Variants in *ELOVL4* are associated with three Mendelian disorders: autosomal dominant (AD) Stargardt-like macular dystrophy type 3, AD spinocerebellar ataxia, and autosomal recessive disorder congenital ichthyosis, spastic quadriplegia and impaired intellectual development (ISQMR). Only seven subjects from five unrelated families with ISQMR have been described, all of which have biallelic single-nucleotide variants.

This is an open access article under the terms of the [Creative Commons Attribution-NonCommercial-NoDerivs](https://creativecommons.org/licenses/by-nc-nd/4.0/) License, which permits use and distribution in any medium, provided the original work is properly cited, the use is non-commercial and no modifications or adaptations are made.

© 2023 The Authors. *Molecular Genetics & Genomic Medicine* published by Wiley Periodicals LLC.

Methods: We performed clinical exome sequencing on probands from four unrelated families with neuro-ichthyosis.

Results: We identified three novel homozygous *ELOVL4* variants. Two of the families originated from the same Saudi tribe and had the exact homozygous exonic deletion in *ELOVL4*, while the third and fourth probands had two different novel homozygous missense variants. Seven out of the eight affected subjects had profound developmental delay, epilepsy, axial hypotonia, peripheral hypertonia, and ichthyosis. Delayed myelination and corpus callosum hypoplasia were seen in two of five subjects with brain magnetic resonance imaging and cerebral atrophy in three.

Conclusion: Our study expands the allelic spectrum of *ELOVL4*-related ISQMR. The detection of the same exonic deletion in two unrelated Saudi family from same tribe suggests a tribal founder mutation.

KEYWORDS

autosomal recessive, copy number variant, *ELOVL4*, neuro-ichthyosis

1 | INTRODUCTION

Neurocutaneous syndromes are a heterogeneous group of disorders characterized by skin and central nervous system involvement and are mainly genetic in nature (Fischer & Bourrat, 2020). One particular group of these disorders are neuro-ichthyoses in which there is dryness and scaling of skin with variable neurological manifestations (Rizzo et al., 2012). Over the past decade and with the application of next-generation sequencing, the genetic basis of neuro-ichthyoses has been increasingly recognized and a variety of pathways including those involved in lipid metabolism, glycoprotein synthesis, or intracellular vesicle trafficking have been implicated (Rizzo et al., 2012).

Very long-chain fatty acids (VLCFAs) are fatty acids with more than 22 carbon atoms. VLCFAs can be divided into saturated, monounsaturated, and polyunsaturated fatty acids (Leonard et al., 2004), all of which are important for maintaining the structure and function of cell membranes (Schneider et al., 2004). VLCFAs play a unique role in the brain, retina, and skin (Agbaga, 2016). They are synthesized by a multiprotein elongation system referred to as the ELOVL group (Beaudoin et al., 2009). Elongation of very long-chain fatty acids-4 (*ELOVL4*) is a member of the ELOVL group that is responsible for fatty acid elongation and is the only member that catalyzes production of VLCFAs and very long-chain polyunsaturated fatty acids (VLC-PUFAs) of 28 carbon atoms and more, with the highest expression of *ELOVL4* in the brain, retina, and skin (Deák et al., 2019; Vasireddy et al., 2007).

Until now, pathogenic variants in *ELOVL4* have been associated with three different Mendelian disorders with

variable neurological, ophthalmological, and cutaneous manifestations and different modes of inheritance (Deák et al., 2019). The first disease is Stargardt-like macular dystrophy type 3 (STGD3) (MIM #600110), an autosomal dominant (AD) disorder caused by heterozygous pathogenic variants in *ELOVL4* that presents with isolated juvenile visual loss (Agbaga et al., 2008). The second is an AD disorder caused by heterozygous pathogenic variants in *ELOVL4* resulting in spinocerebellar ataxia 34 with erythrokeratoderma (SCA34) (MIM#133190) which consists of ataxia, incoordination, visual problems, dysarthria, and skin involvement (Bourassa et al., 2015; Sullivan et al., 2019). The third and most rare disorder associated with *ELOVL4* is ichthyosis, spastic quadriplegia, and impaired intellectual development (ISQMR; MIM #614457) which has an autosomal recessive (AR) inheritance (Aldahmesh et al., 2011; Diociaiuti et al., 2021; Mir et al., 2014). Patients with ISQMR exhibit features of ichthyosis, seizures, intellectual disability, and spasticity (Rizzo et al., 2012), although isolated congenital ichthyosis without neurological involvement has also been described in one family (Mir et al., 2014).

To date, only seven cases with ISQMR from five unrelated families have been described; five of these cases share almost the same clinical features of profound developmental delay, seizures, and congenital ichthyosis (Aldahmesh et al., 2011; Diociaiuti et al., 2021; Mir et al., 2014).

Here, four new families with ISQMR were reported, including two families originating from the same Saudi tribe with a novel homozygous exonic deletion in *ELOVL4*, possibly representing a founder allele. Our cases expand the

genotypic spectrum of ISQMR and highlight the contribution of small copy number variants (CNVs) in the pathogenesis of rare Mendelian disorders.

2 | METHODS

Informed consent for publication of relevant findings and clinical photographs was obtained from the legal guardians of the affected individuals from all families. The research study was approved by the Research and Ethical Committee of the Ministry of Health in Kuwait and King Faisal Specialist Hospital and Research Center and was conducted according to the ethical principles of Declaration of Helsinki. The proband from Family 4 was previously published with limited clinical information (Monies et al., 2017).

2.1 | Genetic testing

Proband clinical exome sequencing (cES) was performed on the proband from all families. cES of the index cases from Families 1 and 2 was performed at an accredited diagnostic company (CENTOGENE GmbH), and cES for the index of Family 3 and 4 was performed in a local Clinical Laboratory Improvement Amendments (CLIA)-certified genetic laboratory. All variants are described according to transcript NM_022726.3.

DNA was extracted from ethylenediamine tetracetic acid blood or from dried blood spots (DBSs) on filter cards (CentoCard®) with QIASymphony using a magnetic bead-based method (Qiagen), with an acceptance criterion of minimum 3 ng/μL. Genomic DNA is enzymatically fragmented, and target regions are enriched using DNA capture probes. These regions include approximately 41 Mb of the human coding exome (targeting >98% of the coding RefSeq from the human genome build GRCh37/hg19), as well as the mitochondrial genome. The generated library is sequenced on an Illumina platform to obtain at least 20× coverage depth for >98% of the targeted bases. An in-house bioinformatics pipeline, including read alignment to GRCh37/hg19 genome assembly and revised Cambridge Reference Sequence (rCRS) of the Human Mitochondrial DNA (NC_012920), variant calling, annotation, and comprehensive variant filtering, is applied. All variants with minor allele frequency (MAF) of less than 1% in gnomAD database, and disease-causing variants reported in HGMD®, in ClinVar or in CentoMD® are evaluated. The investigation for relevant variants is focused on coding exons and flanking ±10 intronic nucleotides of genes with clear gene-phenotype evidence (based on OMIM® information). All potential patterns for mode of

inheritance are considered. In addition, family history and clinical information are used to evaluate identified variants with respect to their pathogenicity and disease causality. Variants are categorized into five classes (pathogenic, likely pathogenic, variant of unknown significance, likely benign, and benign) along American College of Medical Genetics guidelines for the classification of variants. The CNV detection software has a sensitivity of more than 95% for all homozygous/hemizygous and mitochondrial deletions, as well as heterozygous deletions/duplications and homozygous/hemizygous duplications spanning at least three consecutive exons.

Quantitative polymerase chain reaction (QPCR) reactions were performed on individuals from Family 1 (proband [Subject S1] and parents) and Family 2 (proband [Subject S2], affected siblings [Subjects S3 and S4], and parents) using the SensiMix™ SYBR® No-ROX Kit (Bioline), on LightCycler® 480 II (Roche) system. Gene-specific primers encompassing coding exons 1 and 2 (or part of it) of *ELOVL4* based on transcript NM_022726.3. The primer design was as follows:

Exon 1 forward (5' → 3') primer: GTGTCCTAAACGTA GTGTCCAC

Exon 1 reverse (5' → 3') primer: GAAGTCAGCGGCTT TACCTG

Exon 2 forward (5' → 3') primer: AATTGGCCTCTGAT GCAGTC

Exon 2 reverse (5' → 3') primer: AAAGGTTCTCGGTC CTTCATCC

Additionally, multiple gene-specific primers encompassing coding exons 1 and 2 of *ELOVL4* as well as the upstream region were designed for long-range PCR to determine the breakpoint junction. The design was as follows:

Exon 1 forward primer 1: caccacgcctacctcatctt

Exon 1 reverse primer 1: gaggggaggccttaacattc

Upstream forward primer: ttgcttggttcattccatgtat

Upstream reverse primer: gaagaatgggtgttctgtgg

Exon 2 forward primer: tgggactcaaaggacagtga

Exon 2 reverse primer: caatgatggtttacacattctca

Exon 1 forward primer 2: ttcatgcaattatatgttgattgtt

Exon 1 reverse primer 2: ggagatgtgggagcacagg

Upstream forward primer 2: tgtgaaggcaggaacaat

Upstream reverse primer 2: tcgaccatgaacaaatcaa

2.2 | Biochemical tests

Very long-chain fatty acid-containing lysophosphatidylcholine (LysoPC) analysis was performed on DBSs from

the proband from Family 3 (subject S5) and proband of Family 4 (Subject S7) according to the method previously described after adaptation of the multiple reaction monitorings to also measure the abundance C28:0-LysoPC in addition to C26:0-LysoPC (Jaspers et al., 2020). The C28:0-lysoPC concentration was calculated using the deuterium-labeled C26:0-LysoPC internal standard assuming identical response.

2.3 | Clinical reports

2.3.1 | Family 1 (Subject S1)

The proband is a 2-year-old Saudi boy who is the first child of a non-consanguineous couple from the same tribe (Figure 1a). He was delivered by cesarean section with a birth weight of 3.180 kg following an uneventful pregnancy. Activity, pulse, grimace, appearance and respiration scores were 7 and 9 at 1 and 5 min, respectively. He was admitted to the neonatal intensive care unit (NICU) for 1 week after the team noticed he had shiny, dry, and scaly

skin. He was diagnosed with ichthyosis and prescribed topical emollients by a dermatologist. An echocardiogram was done as part of screening for associated congenital anomalies which showed patent ductus arteriosus (PDA) and atrial septal defect (ASD) secundum. At the age of 4 months, his mother brought him to medical attention due to poor feeding and episodes of cyanosis. He was admitted to the hospital in Saudi Arabia and was noted to be dehydrated. Workup showed evidence of hypernatremia (sodium level of 151 mmol/L). He was diagnosed with gastroesophageal reflux disease (GERD) and was discharged after 4 days following rehydration with intravenous fluids and initiation of proton pump inhibitors. Follow-up echocardiogram during hospitalization was normal. The episodes of cyanosis continued and were associated with tonic stiffening of limbs for 10–15 s. He was later diagnosed with seizures and started on phenobarbitone.

At 13 months of age, he presented with uncontrolled seizures in the form of recurrent episodes of tonic stiffening lasting for 10–15 s, and levetiracetam was added to his antiepileptic medication regimen. Thorough general and neurological examinations were performed, and he

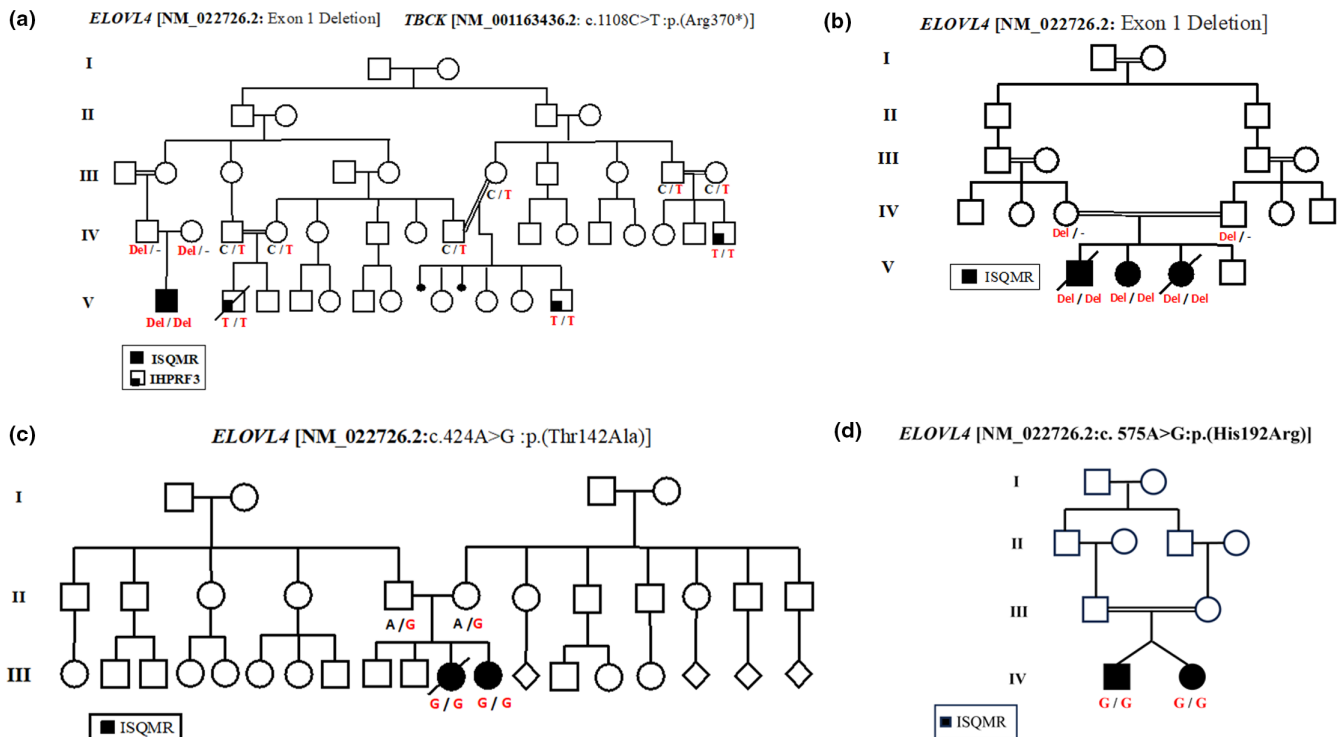


FIGURE 1 Pedigrees of families 1–4. (a) Extended 5-generation pedigree of the proband of Family 1. Note that two autosomal recessive neurodevelopmental disorders have been detected in this family and confirmed to be caused by two different genes accounting for the intrafamilial variability. (b) Extended 5-generation pedigree of Family 2. Note the single loop of consanguinity as the parents are second-degree cousins. The black-colored square and circles depict the affected children in the family. (c) A 3-generation pedigree of Family 3 showing the proband's extended family members, her two healthy older brothers, and her youngest affected sister. The proband and her younger affected sister are depicted with black-colored circle. (d) A 4-generation pedigree of Family 4 showing the proband and his affected twin sibling which are products of a first-degree cousin marriage. The proband and his affected twin sister are depicted in black-colored squares.

was also noted at that time to have profound global developmental delay (GDD), microcephaly, and failure to thrive. At 13 months of age, he was unable to support his neck, turn, or sit independently. He could not fix or follow and had no social smile. He was unable to recognize his parents and had never produced any sounds. His anthropometric measurements were as follows: head circumference of 45.5 cm (2nd %tile for age), 6.7 kg (<1st %tile for age) of weight, and 79 cm (<1st %tile for age) of height. He also had strabismus and mild dysmorphic features including epicanthal folds and triangular face. His skin was dry, scaly, and erythematous, and he had seborrheic dermatitis on his scalp (Figure 2Ai–iii). Neurological examination showed severe axial hypotonia with poor head control,

peripheral hypertonia with fistled hands, contractures, and scissoring of his legs. His reflexes were brisk throughout. Additionally, he had abdominal distension, but there was no evidence of organomegaly to suggest a storage disease.

From age 13 months to 2 years, he had recurrent hospitalization and pediatric intensive care unit admissions due to acute exacerbation of asthma and aspiration pneumonias with severe respiratory distress. His skin changes and seborrheic dermatitis on his scalp never resolved. Family history was significant for two second cousins with profound developmental delay and hypotonia (Figure 1a) and a previous diagnosis of infantile hypotonia with psychomotor retardation and characteristic facies type 3 (MIM# 616900) due to a likely pathogenic homozygous variant

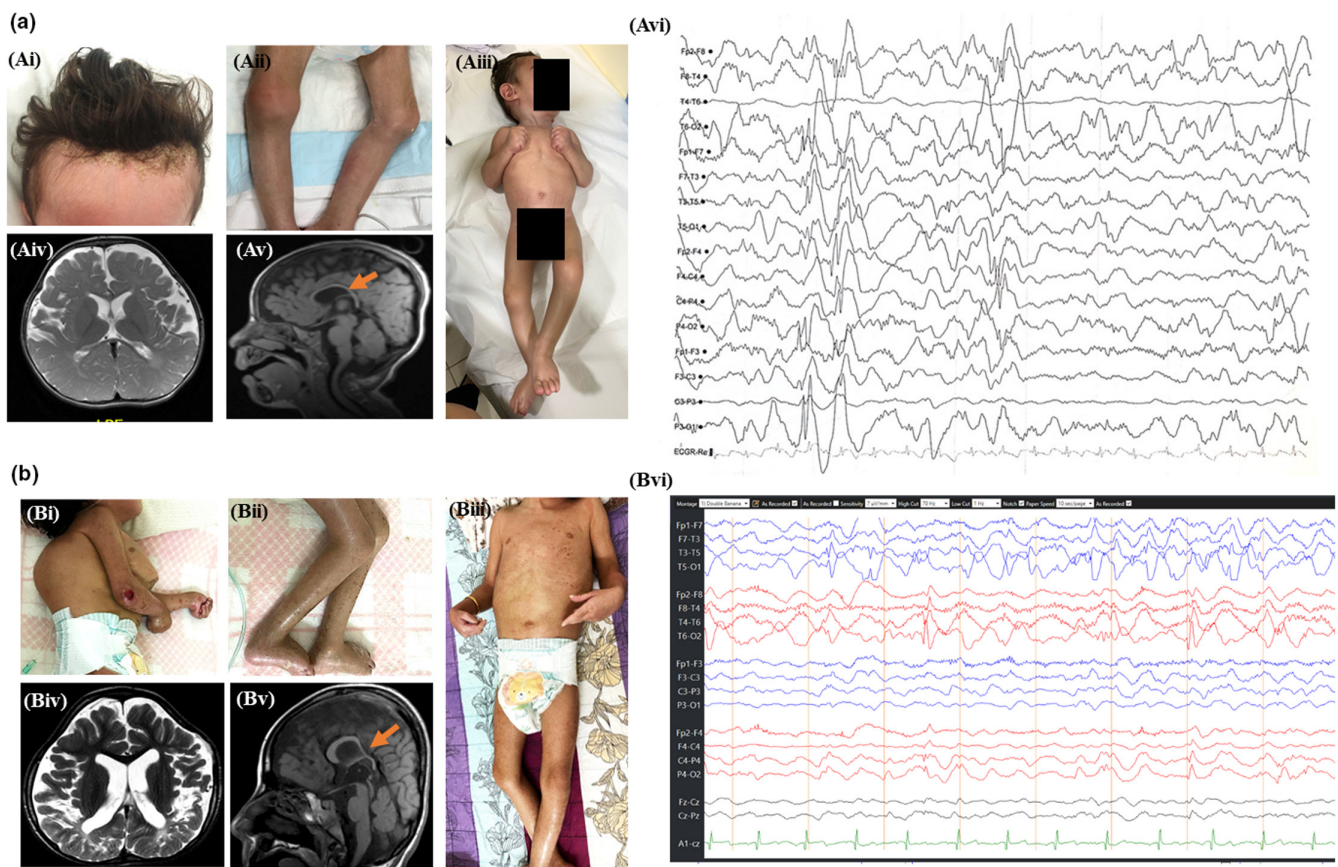


FIGURE 2 Photos and magnetic resonance imaging (MRI) and electroencephalogram (EEG) images of patients from Families 1 and 2. (Ai–Aiii) Photographs of proband of Family 1 (Subject S1) showing seborrheic dermatitis of the scalp, limb contractures, and ichthyosis. (Aiv–Av) MRI brain (axial T2-weighted and sagittal T1-weighted images) of proband of Family 1 (Subject S1) showing diffuse cerebral volume loss, delayed myelination for age, and thin corpus callosum (orange arrow). (Avi) A screenshot of the proband's (Family 1/Subject S1) EEG 10-second epoch (bipolar montage; sensitivity 15 μ V/mm) showing slow background and multifocal epileptiform activity. (Bi–Bii) Photograph of proband's first sister of Family 2 (V-2, Subject S3) showing chest deformity, ulcerative skin lesions, dry shiny skin in the lower limbs with skin peeling, and contractures. (Bii) A photograph of the proband's second sister (V-3) of Family 2 (Subject S4) showing dry shiny skin. (Biv–Bv) MRI brain (axial T2-weighted and sagittal T1-weighted images) of proband of Family 2 (V-1, Subject S2) shows ulegyria, volume loss, and abnormal hyperintensity in the parietooccipital white matter and of the depths of the sulci, diffuse atrophy, and marked thinning of the body and splenium of the corpus callosum (orange arrow). No atrophy of the cerebellum or brainstem. (Bvi) A screenshot of the proband's first sister's (Subject S3's) EEG 10-second epoch (bipolar montage; sensitivity 7 μ V/mm) showing bilateral independent posterior spike slow wave discharges seen bilaterally but more on the right side. There is also poorly formed and poorly organized background. Findings are suggestive of epileptic encephalopathy with epileptiform discharges more abundant in the right hemisphere.

in *TBCK* [NM_001163436.2: c.1108C>T: p.(Arg370*)]; however, these two cousins lacked the skin findings and had a less severe course of illness. *TBCK* encodes a TBC1 domain-containing kinase (TBCK). The patient had extensive investigations and workup which included normal plasma amino acids and urine organic acids levels. VLCFA was ordered but was not available. His awake and asleep electroencephalogram (EEG) recording at 9 months of age was abnormal with diffuse delta background slowing and frequent multifocal epileptiform discharges over the left frontocentral, left occipital, right frontocentral, and right temporooccipital regions. Brain magnetic resonance imaging (MRI) was performed at 9 months of age and showed diffuse cerebral atrophy and thin corpus callosum with no evidence of structural abnormalities (Figure 2Aiv–v). He was also referred twice for detailed ophthalmological exam, visual evoked potential (VEP), and electro-retinography, but none were performed due to lack of follow-up.

Local neurology panel at the Kuwait Medical Genetic Centre was negative. The panel included *SNAP29* but did not include *TBCK* nor other genes associated with neuroichthyosis such as *ALDH3A2*, *APIB1*, *ELOVL4*, *DOLK*, and *SUMF1*. A chromosomal microarray (CMA) with both microarray-based comparative genomic hybridization (aCGH) and single-nucleotide polymorphism (SNP) performed showed three long contiguous stretches of homozygosity greater than 10 Mb on chromosomes 6, 12, and 14 [arr [hg19] 6p13q14.1 (71,076,993–82,660,403), 12q22q23 (95,579,058–106,514,145), and 14q13.1q21.2 (34,449,999–45,157,248)] indicating parental consanguinity. Given the clinical presentation which was different from that in his second cousins with a homozygous *TBCK* variant, the severity of his condition, the possibility of dual molecular or alternative diagnoses, and the implication for future pregnancies, a decision was made to proceed with exome sequencing.

2.3.2 | Family 2 (Subjects S2–S4)

The proband (V-1, Subject S2) in this family is a Saudi male who died at 6 years of age and who originated from the same tribe as proband from Family 1 but was apparently unrelated. His parents are first-degree cousins, and he had three younger siblings including two similarly affected sisters and one healthy brother (Figure 1b). He was born prematurely at 32 weeks of gestation, and the pregnancy was complicated by oligohydramnios and meconium-stained amniotic fluid. He was admitted to the NICU for 3 months and was mechanically ventilated for acute respiratory distress syndrome. After he was discharged, he had multiple hospital admissions due to recurrent chest infections,

aspiration pneumonia, and during one admission, he had a cardiac arrest. During his multiple hospitalizations, he was found to have spastic quadriplegia, profound GDD, drug-responsive epilepsy (controlled with valproic acid), and generalized ichthyosis, and the possibility of Sjogren–Larsson syndrome was raised. He was also diagnosed with GERD after repeated vomiting and failure to thrive and underwent fundoplication and gastric tube placement for feeding.

At 4 years of age, he presented to the hospital for severe respiratory distress and was transferred to intensive care unit for respiratory support. His workup included an echocardiogram and abdominal ultrasounds which were normal. MRI brain showed generalized cerebral atrophy and marked thinning of the body and splenium of the corpus callosum (Figure 2Biv–v). His abdominal computerized tomography scan showed mild splenomegaly, multiple bilateral renal stones with hydronephrosis and perinephritic inflammatory changes suggestive of chronic inflammation, bilateral atelectasis, and bronchiectasis, incidentally, noted bilateral inguinal hernia and significant muscle wasting and right hip dislocation. He never had a detailed ophthalmological exam, nor VEP or electroretinogram (ERG). Plasma amino acids, urine organic acids, and carnitine and acylcarnitine levels were unremarkable. He had a skin biopsy performed on his right upper arm as part of workup for ichthyosis which showed epidermal hyperkeratosis, hypergranulosis, acanthosis, spongiosis, and nonspecific dermal inflammation with no evidence of porokeratosis, granuloma annulare, psoriasis, or fungal infection. The overall findings were thought to be nonspecific but possibly suggestive of Netherton syndrome. He became ventilator-dependent and was transferred to the pediatric long stay unit and managed with rehabilitation care for 2 years. He was assigned “do not resuscitate status” and eventually passed away in the hospital at 6 years of age.

The first affected sibling (V-2, Subject S3) is a female who is now 5 years old with GDD and drug-responsive epilepsy. Her seizures are controlled with levetiracetam and carbamazepine. She has the same cutaneous features of the proband in the form of skin dryness and scaling (Figure 2Bi–ii). Her neurological examination shows inability to fix or follow, generalized hypotonia, and exaggerated deep tendon reflexes. Her routine EEG demonstrates poorly organized slow background activity that is mainly in the delta-theta range with repeated electro-decrements bilaterally. She never had detailed eye exam, VEP, or ERG.

The second and youngest affected sibling (V-3, Subject S4) is a 4-year-old female with severe GDD, axial hypotonia, peripheral hypertonia, drug-responsive epilepsy, and congenital ichthyosis (Figure 2Biii). Her seizures are controlled with levetiracetam. Her skin findings were noticed

soon after birth which manifested as colloid membrane that progressed to ichthyosis. Her development is profoundly delayed as she cannot produce any sounds or hold her head up, and she has limited social interaction. Her awake and sleep routine EEG showed poorly organized background rhythm in the delta-theta range with mild asymmetry on the right. She also had frequent bursts and runs of 2 Hz spikes and slow wave activity bilateral raising the concern for epileptic encephalopathy. Detailed ophthalmological exam, VEP, and ERG were never performed. The child died at 4 years of age due to a respiratory infection that led to respiratory failure.

2.3.3 | Family 3 (Subjects S5-S6)

The proband in this family (Subject S5) is a Pakistani female who died at 6 years of age. Her parents are unrelated but come from the same small town (Figure 1c). She has two healthy brothers and one similarly affected younger sister. She was born at 38 weeks following an uncomplicated pregnancy via emergency cesarean section due to fetal deceleration. Prenatal ultrasound was normal with normal amniotic fluid volume. After delivery, the proband had extremely dry, scaly erythematous skin which improved with emollients. She developed her first seizure at the age of 3 months after vaccination. She had drug-resistant epilepsy with daily seizures and was diagnosed with early-onset epileptic encephalopathy with multiple seizure types as well as GDD. She had failure to thrive as her weight, height, and head circumference were all on the 0.4th percentile for age. She received her feeds by a gastrostomy tube. She had coarse dysmorphic features with synophrys, long eye lashes, and pectus excavatum. The cutaneous features included dry, scaly skin, and severely erythematous skin lesions. She had abnormal neurological examination with axial hypotonia. Her ophthalmological examination demonstrated cone-rod macular dystrophy and possible optic disc atrophy associated with severe visual impairment. Her brain MRI at 1 year of age was normal. Her EEG at 5 years of age showed hypsarrhythmia.

The proband's affected younger sister (Subject S6) is a 2-month-old girl who was born at term by spontaneous vaginal delivery. There was no history of colloid membrane or skin shedding at birth, but skin dryness and skin thickening were noted. She was evaluated at 2 months of age in the genetics clinic at which time her examination was normal apart from the skin ichthyosis. She also had normal developmental milestones up to her current age of 2 months as she was able to smile and track. Her neurological examination was also normal. EEG and brain MRI were not performed, given she had normal

neurological examination with no history of seizures. She never had ERG or VEP, given no concern about her vision at 2 months of age.

2.3.4 | Family 4 (Subjects S7-S8)

This proband (Subject S7) from this family was previously published as subject 16-2552 (Monies et al., 2017). He was 8 months old at last examination and was a product of a consanguineous marriage and part of a twin pregnancy. He was born preterm at 34 weeks of gestation and was admitted to the NICU for 20 days for respiratory support. He had ichthyosis since birth. He started having seizures at the age of 6 months, and they were generalized tonic-clonic in nature and were eventually controlled with two anticonvulsant medication (levetiracetam and phenobarbital). With time, he was noted to have GDD. He underwent corrective surgery of bilateral inguinal hernia at 6 months of age. He had recurrent hospital admissions for acute exacerbation of asthma, pneumonia, or bronchiolitis. He had GERD and feeding difficulties and receives his feeds by nasogastric tube (NGT). His examination at the age of 8 months showed failure to thrive; his weight was 3.65 kg (<1st %tile for his age), height was 54 cm, and head circumference was 39 cm (<3rd %tile for his age). He has fair skin and blond-gray thin hair, and his skin was scaly and dry. His neurological examination showed hypotonia and spasticity in all limbs. He was inattentive and had poor fixing and following. His fundus examination revealed bitemporal pallor of the optic disks mostly due to central lesion suggestive of optic atrophy. Complete blood count, renal profile, hepatic profile, and random glucose were normal. He also had normal urine creatinine (5180 $\mu\text{mol/L}$), urine creatinine LC (7380 $\mu\text{mol/L}$), urine guanidinoacetate (1071 $\mu\text{mol/L}$), and urine creatine/creatinine LC ratio (0.702). DBSs acylcarnitine profile and urine gas chromatography-mass spectrometry (GC-MS) were also unremarkable. Biotinidase level was slightly low at 3.8 nmol/min/mL. Barium swallow showed repeated episodes of tracheal aspiration with no cough reflex, otherwise normal upper gastrointestinal barium swallow study. EEG was abnormal with abundant epileptic discharges arising from the posterior head region with disorganized background. A myoclonic jerk of the upper extremity was captured during the routine EEG and was associated with attenuation of background. Echocardiography was normal, and abdominal ultrasound showed mild diffuse increased liver parenchymal echogenicity with borderline size to mild enlargement and no focal lesions. MRI brain done at the age of 8 months was normal. Chromosomal microarray analysis (CGH array) showed no definitely pathogenic CNVs.

The proband's twin (Subject S8) in a female that has similar phenotypic features except the MRI brain shows moderate diffuse brain atrophy predominantly in frontal lobe.

3 | RESULTS

For Family 1, proband cES (on subject S1) did not identify any causative single-nucleotide variants (SNVs). CNV analysis from unphased exome data identified a novel homozygous deletion in the first exon of approximately 649 bp, in *ELOVL4* [Chr6:80656887–80657532 (hg19): NM_022726.3] (Figure 3). The detected CNV in *ELOVL4* was not present in publicly available control databases (Atherosclerosis Risk in Communities, ARIC; Grand Opportunity Exome Sequencing Project, GO-ESP; 1000 Genomes Project; and the genome aggregation database, gnomAD) or in CENTOGENE bio/databank (600,000 exomes) in either the homozygous or heterozygous state. QPCR confirmed the homozygosity for exon 1 deletion in the proband from Family 1 and heterozygosity in both

parents consistent with Mendelian expectations. *ELOVL4* falls within one of three long regions of homozygosity (>10 Mb) detected by SNP array [6p13q14.1 (71,076,993–82,660,403)]. Interestingly, review of the array CGH data showed *ELOVL4* is covered with six probes, and a small homozygous 5.14 Kb CNV in *ELOVL4* was observed but was below the threshold for reporting (Figure 3). Both microarray and exome data showed normal copy number of exons 2–6 of *ELOVL4* (Figure 3), suggesting that the first break point of this deletion could be located in intron 1 (15.5 Kb) of *ELOVL4*. Additionally, in the microarray data, a probe upstream *ELOVL4* showed normal copy number 25.6 Kb away from the deletion. This indicates that the second break point is within the 25.6-Kb intergenic region. Both of these regions contain a number of repeat sequences. One of the suggested mechanisms for the formation of such a small deletion is from non-allelic homologous recombination (NAHR). Low-copy repeats sequence trigger recombination and result in copy number variation (McDonald-McGinn et al., 2015). Sequences that trigger NAHR may be present in the two areas where the suspected break points fall. Several attempts to map the

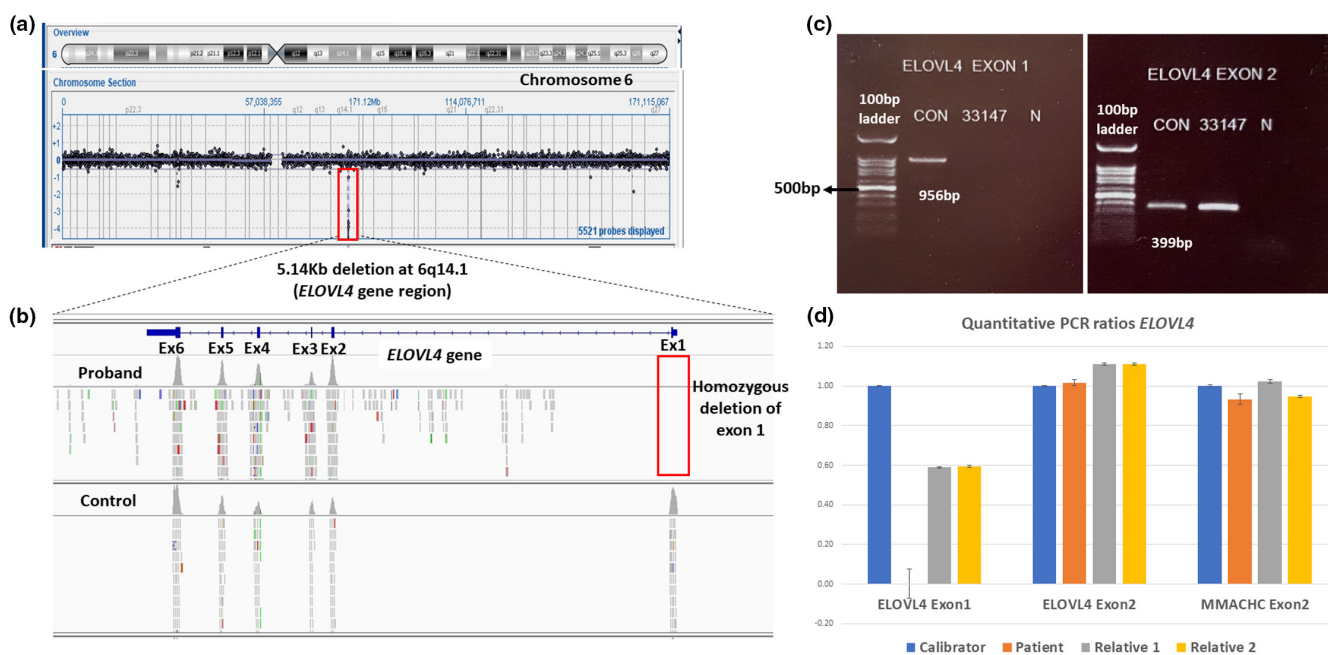


FIGURE 3 Genomic data from proband of Family 1 (Subject S1) including array CGH and BAM files around the deletion and PCR confirmation. (a) A microarray result of 5.14 Kb deletion (Chr6:80652752–80657887) involving exon 1 of *ELOVL4* in the proband from Family 1 (Subject S1) is shown. The image was obtained from microarray *CytoSure® Interpret Software, Oxford Gene Technology*. (b) Whole-exome sequencing of the same proband from Family 1 (Subject S1) which show no coverage of exon 1 of *ELOVL4* indicating there is homozygous deletion of exon 1. As for the control samples of the same region, the coverage of exon 1 was observed. The image was obtained from Integrative Genomics Viewer (IGV) bam files of the proband and a control. (c) Polymerase chain reaction (PCR) was used to amplify both exon 1 and 2 of *ELOVL4*. (Left side) No amplification of exon 1 in the proband from Family 1 (33147) was detected; however, there is amplification in control (product size: 956 bp). (Right side) Amplification of exon 2 of *ELOVL4* was successful in both control and proband from Family 1 (33147) (product size: 399 bp). (d) Real-time PCR of proband from Family 1 (Subject S1) targeting *ELOVL4* exon 1, *ELOVL4* exon 2, and reference gene *MMACHC* exon 2 is shown. The graph shows the ratio of the quantitative PCR, patient in orange, control sample in blue, and two relative samples (unaffected parents).

breakpoint junction with long-range PCR using primers described in the methods failed to amplify the region. The size of the regions where the suspected break points fall are large and contain a number of repeat sequences, making the process of mapping the break points challenging.

For Family 2, cES was carried out in the proband (Subject S2) and did not identify any potential SNVs to explain the phenotype. CNV analysis from unphased exome data identified the same novel homozygous *ELOVL4* deletion detected in the proband from Family 1 [Chr6:80656887–80657532 (hg19): NM_022726.3]. Subsequent QPCR analysis for the suspected deletion confirmed homozygosity in the proband from Family 2 as well as his affected sisters (Subjects S3–S4) and heterozygosity in his parents co-segregating with the disease. VLCFA (by GC–MS) in the youngest affected sister was normal: behenic acid (C22:0) 83 $\mu\text{mol/L}$, lignoceric acid (C24:0) 55.9 $\mu\text{mol/L}$, cerotic acid (C26:0) 0.5 $\mu\text{mol/L}$, C24/C22 ratio 0.67, C26/C22 ratio 0.01, phytanic acid 1.46 $\mu\text{mol/L}$, and pristanic acid <0.14 $\mu\text{mol/L}$.

In Family 3, cES on the proband (Subject S5) identified a novel homozygous missense variant c.424A>G; p.(Thr142Ala) in *ELOVL4*. This variant is ultrarare and is not present in gnomAD or in CENTOGENE bio/databank. Segregation study showed that the parents were heterozygous and youngest affected sister (Subject S6) was also homozygous for the variant conforming with Mendelian expectations for AR. In silico predictions were

categorized as damaging (Polyphen, MutationTaster, SIFT, with a high CADD). C26:0-lysoPC analysis in fibroblasts showed slightly elevated levels of 16 pmol/ μgram protein (ref. 2–14). D3-C22 loading in fibroblasts to ascertain both VLCFA β -oxidation capacity and elongation was normal with a D3-C26 level (elongation) of 0.29 (ref. 0.15–0.51) and D3-C16/D3-C22 ratio (β -oxidation) of 1.17 (ref. 0.88–1.93). Additional LysoPC testing in DBSs from the proband of Family 3 (Subject S5) was performed to measure C26:0- and C28:0-lysoPC for the proband, which showed normal C26:0-lysoPC levels but low C28:0-lysoPC levels and a clearly lowered C28/26 ratio when compared to controls (Figure 4).

In Family 4, cES in the proband (Subject S7) identified a novel homozygous missense variant [NM_022726:c.575A>G;p.(His192Arg)] in *ELOVL4*. C26:0- and C28:0-LysoPC as well as the ratio showed a similar pattern as observed for subject S5 (Figure 4).

4 | DISCUSSION

We report four unrelated families with novel homozygous *ELOVL4* variants and ISQMR. Three of these families originated from Saudia Arabia, and two of them from the same Saudi tribe and carried a novel homozygous exonic deletion in the first coding exon of *ELOVL4*, while the probands from the third and fourth family were

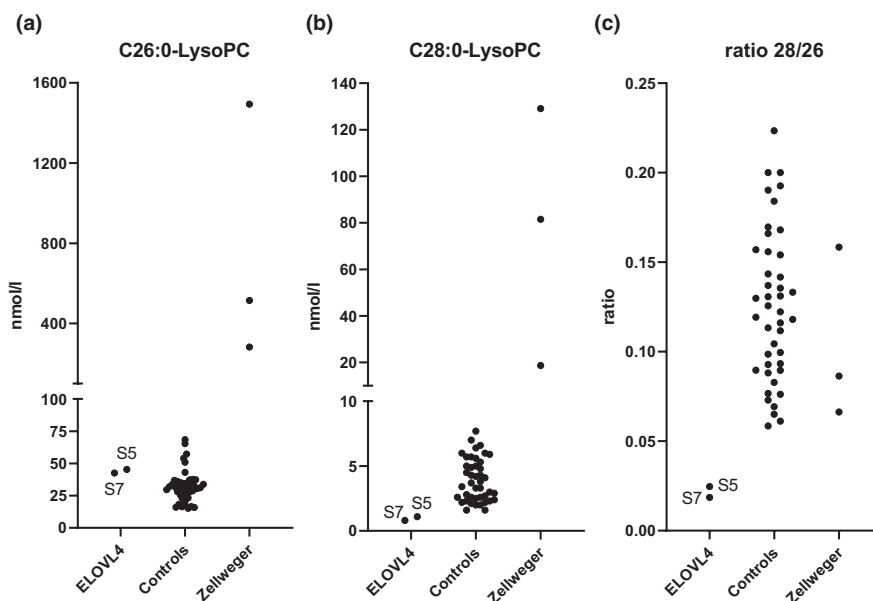


FIGURE 4 Very long-chain fatty acid-containing LysoPC levels (C26:0, C28:0) in subject S5 (Family 3) and subjects S7 (Family 4) with ISQMR compared to control and subjects with Zellweger syndrome (ZS). (a) Measurements of C26:0-LysoPC in dried blood spots in subjects S5 (Family 3 proband) and S7 (Family 4 proband) show that the C26:0-LysoPC level is normal in both. (b) Measurements of C28:0-LysoPC in dried blood spots in subjects S5 (Family 3 proband) and S7 (Family 4 proband) show that the C28:0-LysoPC level is reduced in both. (c) Measurement of C28/26 ratios in dried blood spots in subjects S5 (Family 3 proband) and S7 (Family 4 proband) show that C28/C26 ratio is reduced in both subjects compared to controls and subjects with ZS.

homozygous for a novel missense variant. Only five families with *ELOVL4* SNVs have been reported to date, and no patients with a homozygous CNV involving *ELOVL4* have been published so far (Pubmed, HGMD, Decipher).

Table 1 summarizes the demographic, variant information, and investigations in all subjects with biallelic *ELOVL4* variants reported to date. **Table 2** summarizes the clinical features observed in all subjects with biallelic *ELOVL4* variants reported to date. Our subjects have cutaneous, neurological, and ophthalmological features, consistent with the features in previously reported patients.

The cutaneous features mostly resemble those seen in the seven previously reported cases with *ELOVL4* variants (Aldahmesh et al., 2011; Diociaiuti et al., 2021; Mir et al., 2014). Three out of the seven published cases first presented with colloid membrane soon after birth. A colloid membrane was also observed after birth in two out of six subjects in our study (Family 2), while this information was not available in one family (Family 1). All our subjects had skin signs from early infancy, presenting during the neonatal period with thick, dry, and scaly skin suggestive of ichthyosis. All the reported cases with biallelic *ELOVL4* variants to date have had the same cutaneous findings of dry and scaly ichthyotic skin. Erythema of the skin has also been noted in five out of the eight subjects in our study. The proband from Family 1 also has seborrheic dermatitis of the scalp that persisted until the current age of

2 years which had not been described in any of the previously reported cases.

In addition, majority of our subjects had similar findings such as failure to thrive (7/8), profound GDD (7/8), epilepsy (7/8), axial hypotonia (6/7), and peripheral hypertonia (5/6), which were reported in all but two cases with biallelic *ELOVL4* variants. The two cases were from same family (Family 7 in **Tables 1** and **2**) and had skin manifestations but lacked the additional neurological findings (Mir et al., 2014). This intrafamilial variability is striking but was not seen in the multiplex family (Family 2) in this report. However, Subject S6 from Family 3 has a normal neurological examination until now but will be closely followed up to monitor for any new neurological manifestation. Epilepsy was drug-resistant in minority of our subjects (2/7), and epileptiform activity was observed in 4/5 of our subjects who had an EEG. A study on homozygous knock in mice for the STGD3-causing *ELOVL4* mutations, with skin-specific rescue of wild-type *ELOVL4* expression to avoid neonatal lethality due to dehydration, showed that the mice had seizures postnatally. These mice had evidence of spontaneous epileptiform activity in the hippocampus with aberrant neurotransmission due to dysregulated presynaptic fusion and accelerated neurotransmitter release (Hopiavuori et al., 2018). Although none of the subjects in this study had ataxia, a rat model of *ELOVL4*-related SCA34 showed impaired

TABLE 1 Summary of the demographic data, variant information, and investigations of all subjects with biallelic *ELOVL4* variants to date.

	Family #	This report							
		Family 1	Family 2			Family 3		Family 4	
	Subject #	S1	S2	S3	S4	S5	S6	S7*	
Demographics	Ethnicity	Saudi				Pakistani		Saudi	
	Gender	M	M	F	F	F	F	M	
	Living status (age)	Alive (2yr)	Died (6yr)	Alive (5yr)	Died (4yr)	Died (6yr)	Alive	Alive (8 mo)	
	Consanguinity	+	+			-		+	
	Affected sibling	-	+	+	+	+	+	+	
		CNV				SNV			
Variant Information (NM_022726.2)	Variant type	Exonic deletion (ex 1)				Missense		Missense	
	Zygoty	hmz				hmz		hmz	
	c.DNA	Break points undetermined				c.424A>G		c.575A>G	
	Aminoacid	N/A				p.(Thr142Ala)		p.(His192Arg)	
EEG findings	Slow background	+	N/A	+	+	+	N/A	+	
	Epileptiform activity	+(multifocal)	N/A	-	++ (SSW)	+(Hypsarrhythmia)	N/A	+	
Brain MRI findings	Delayed myelination	+	+	N/A	N/A	-	N/A	-	
	Cerebral atrophy	+	+	N/A	N/A	-	N/A	-	
	Thin CC	+	+	N/A	N/A	-	N/A	-	

Abbreviations: CC, corpus callosum; CNV, copy number variant; Ex, exon; F, female; Hmz, homozygous; M, male; mo, months; N/A, not available; SNV, single-nucleotide variant; SSW, spike and slow wave activity; yr, years, * previous published in Monies et al. (2017)

synaptic plasticity and dysregulation of the cerebellar network which may possibly underline some of the neurological features observed in subjects with ISQMR. Six out of 12 patients reported to date, including our patients, complained of GERD. Swallowing difficulty was also relatively common in six out of the 11 subjects (55%) necessitating nasogastric, orogastric, or gastric tube feeding. Only one of our eight subjects had inguinal hernia which had been previously noted in another subject with ISQMR (Aldahmesh et al., 2011). Dental abnormalities were commonly observed (5/7 cases to date), in the form of delayed teeth eruption (3/7) or tooth loss secondary to gingivitis (1/7), or teeth erosions (1/7). These findings are unexpected, given the low expression of *ELOVL4* in teeth or gum.

Five of eight subjects in our study had brain imaging showing brain atrophy (3/5), delayed myelination (2/5), and thin corpus callosum (2/5), all of which had been observed on brain imaging in three subjects previously reported (Aldahmesh et al., 2011; Diociaiuti et al., 2021; Mir et al., 2014).

Eye findings were uncommon overall, although one major limitation in our current study is the lack of detailed ophthalmological assessment. Retinal screening and VEP were not performed in seven out of the eight subjects in our study. The only subject (proband from Family 3) with detailed eye examination was found to have

cone-rod dystrophy. The proband in Family 1 has myopia and amblyopia as well as a Saudi patient previously reported (Aldahmesh et al., 2011). The proband from Family 4 has optic atrophy similar to subject 15 from Family 10 (Diociaiuti et al., 2021). The two cases from Family 7 in Tables 1 and 2, who only manifested with cutaneous findings, also had abnormal macular changes in their ophthalmological examination like the proband from Family 3 in our study (Mir et al., 2014). Eye findings in the form of macular changes and/or myopia were reported in two parents to date (Aldahmesh et al., 2011; Mir et al., 2014). This is unsurprising given the high expression of *ELOVL4* in the retina, particularly the photoreceptors and association with Stargardt disease (Agbaga et al., 2010). None of the parents in our four families are known to have had visual problems, though they have not had formal eye examination.

ELOVL4 is the only *ELOVL* member responsible for the elongation of VLCFA and VLC-PUFA beyond 28 carbon ($\geq C28$) atoms (Deák et al., 2019; Tvrdik et al., 2000). VLCFA levels were not available on any of the previously published subjects (Aldahmesh et al., 2011; Diociaiuti et al., 2021; Mir et al., 2014). In this study, VLCFA levels were measured for three subjects using GC-MS (Family 2/S3, Family 3/S5 and Family 4/S7) and were normal apart from slightly elevated C26:0 in two of the three subjects. However, C28:0-lyso PC levels of the probands from two

	Aldahmesh et al. (2011)		Mir et al. (2014)			Diociaiuti et al. (2021)		Total
	Family 5	Family 6	Family 7			Family 8	Family 9	
S8	S9	S10	S11	S12	S13	S14	S15	
	Saudi	Indian	Pakistani			Italian		
M	M	M	M	M	F	M	M	
Alive (8 mo)	Alive (6yr)	Died (2yr)	Alive (24yr)	Died (17yr)	Alive (22yr)	Alive (2yr)	Alive (3yr)	
	+	+	+			+	–	8/9
+	–	+(died at 6 mo)	+	+	+	–	–	11/15
	Nonsense	Frameshift	Nonsense			Frameshift	missense	
	hmz	hmz	hmz			hmz	hmz	
	c.646C>T	c.689delT	c.78C>G			c.435dup	c.487T>C	
	p.(Arg216*)	p.(Ile230Metfs*22)	p.(Tyr26*)			p.(Ile146Tyrfs*29)	p.(Cys163Arg)	
N/A	N/A	N/A	N/A	N/A	N/A	+	+	7/7
N/A	N/A	+	N/A	N/A	N/A	+(Hypsarrhythmia)	+(b/l posterior SSW)	7/8
–	+	N/A	N/A	N/A	N/A	+	+	5/8
+	+	N/A	N/A	N/A	N/A	+	+	6/8
–	+	N/A	N/A	N/A	N/A	+	+	5/8

TABLE 2 Summary of the clinical features of all subjects with biallelic *ELOVL4* variants to date.

Family #	This report																		Total																																																																																																																																																																																																																																																																																																																																																																																																																																																																																																																																																																																																																																																																																																																																																																																																																																																																																																																																																																																																																																																																																																																																																																																																																																																																																																																																																																																																																																																																																											
	Family 1			Family 2			Family 3			Family 4			Family 5			Family 6				Family 7			Family 8			Family 9																																																																																																																																																																																																																																																																																																																																																																																																																																																																																																																																																																																																																																																																																																																																																																																																																																																																																																																																																																																																																																																																																																																																																																																																																																																																																																																																																																																																																																																																																				
	S1	S2	S3	S4	S5	S6	S7	S8	S9	S10	S11	S12	S13	S14	S15	S16	S17	S18		S19	S20	S21	S22	S23	S24	S25	S26	S27	S28	S29	S30	S31	S32	S33	S34	S35	S36	S37	S38	S39	S40	S41	S42	S43	S44	S45	S46	S47	S48	S49	S50	S51	S52	S53	S54	S55	S56	S57	S58	S59	S60	S61	S62	S63	S64	S65	S66	S67	S68	S69	S70	S71	S72	S73	S74	S75	S76	S77	S78	S79	S80	S81	S82	S83	S84	S85	S86	S87	S88	S89	S90	S91	S92	S93	S94	S95	S96	S97	S98	S99	S100	S101	S102	S103	S104	S105	S106	S107	S108	S109	S110	S111	S112	S113	S114	S115	S116	S117	S118	S119	S120	S121	S122	S123	S124	S125	S126	S127	S128	S129	S130	S131	S132	S133	S134	S135	S136	S137	S138	S139	S140	S141	S142	S143	S144	S145	S146	S147	S148	S149	S150	S151	S152	S153	S154	S155	S156	S157	S158	S159	S160	S161	S162	S163	S164	S165	S166	S167	S168	S169	S170	S171	S172	S173	S174	S175	S176	S177	S178	S179	S180	S181	S182	S183	S184	S185	S186	S187	S188	S189	S190	S191	S192	S193	S194	S195	S196	S197	S198	S199	S200	S201	S202	S203	S204	S205	S206	S207	S208	S209	S210	S211	S212	S213	S214	S215	S216	S217	S218	S219	S220	S221	S222	S223	S224	S225	S226	S227	S228	S229	S230	S231	S232	S233	S234	S235	S236	S237	S238	S239	S240	S241	S242	S243	S244	S245	S246	S247	S248	S249	S250	S251	S252	S253	S254	S255	S256	S257	S258	S259	S260	S261	S262	S263	S264	S265	S266	S267	S268	S269	S270	S271	S272	S273	S274	S275	S276	S277	S278	S279	S280	S281	S282	S283	S284	S285	S286	S287	S288	S289	S290	S291	S292	S293	S294	S295	S296	S297	S298	S299	S300	S301	S302	S303	S304	S305	S306	S307	S308	S309	S310	S311	S312	S313	S314	S315	S316	S317	S318	S319	S320	S321	S322	S323	S324	S325	S326	S327	S328	S329	S330	S331	S332	S333	S334	S335	S336	S337	S338	S339	S340	S341	S342	S343	S344	S345	S346	S347	S348	S349	S350	S351	S352	S353	S354	S355	S356	S357	S358	S359	S360	S361	S362	S363	S364	S365	S366	S367	S368	S369	S370	S371	S372	S373	S374	S375	S376	S377	S378	S379	S380	S381	S382	S383	S384	S385	S386	S387	S388	S389	S390	S391	S392	S393	S394	S395	S396	S397	S398	S399	S400	S401	S402	S403	S404	S405	S406	S407	S408	S409	S410	S411	S412	S413	S414	S415	S416	S417	S418	S419	S420	S421	S422	S423	S424	S425	S426	S427	S428	S429	S430	S431	S432	S433	S434	S435	S436	S437	S438	S439	S440	S441	S442	S443	S444	S445	S446	S447	S448	S449	S450	S451	S452	S453	S454	S455	S456	S457	S458	S459	S460	S461	S462	S463	S464	S465	S466	S467	S468	S469	S470	S471	S472	S473	S474	S475	S476	S477	S478	S479	S480	S481	S482	S483	S484	S485	S486	S487	S488	S489	S490	S491	S492	S493	S494	S495	S496	S497	S498	S499	S500	S501	S502	S503	S504	S505	S506	S507	S508	S509	S510	S511	S512	S513	S514	S515	S516	S517	S518	S519	S520	S521	S522	S523	S524	S525	S526	S527	S528	S529	S530	S531	S532	S533	S534	S535	S536	S537	S538	S539	S540	S541	S542	S543	S544	S545	S546	S547	S548	S549	S550	S551	S552	S553	S554	S555	S556	S557	S558	S559	S560	S561	S562	S563	S564	S565	S566	S567	S568	S569	S570	S571	S572	S573	S574	S575	S576	S577	S578	S579	S580	S581	S582	S583	S584	S585	S586	S587	S588	S589	S590	S591	S592	S593	S594	S595	S596	S597	S598	S599	S600	S601	S602	S603	S604	S605	S606	S607	S608	S609	S610	S611	S612	S613	S614	S615	S616	S617	S618	S619	S620	S621	S622	S623	S624	S625	S626	S627	S628	S629	S630	S631	S632	S633	S634	S635	S636	S637	S638	S639	S640	S641	S642	S643	S644	S645	S646	S647	S648	S649	S650	S651	S652	S653	S654	S655	S656	S657	S658	S659	S660	S661	S662	S663	S664	S665	S666	S667	S668	S669	S670	S671	S672	S673	S674	S675	S676	S677	S678	S679	S680	S681	S682	S683	S684	S685	S686	S687	S688	S689	S690	S691	S692	S693	S694	S695	S696	S697	S698	S699	S700	S701	S702	S703	S704	S705	S706	S707	S708	S709	S710	S711	S712	S713	S714	S715	S716	S717	S718	S719	S720	S721	S722	S723	S724	S725	S726	S727	S728	S729	S730	S731	S732	S733	S734	S735	S736	S737	S738	S739	S740	S741	S742	S743	S744	S745	S746	S747	S748	S749	S750	S751	S752	S753	S754	S755	S756	S757	S758	S759	S760	S761	S762	S763	S764	S765	S766	S767	S768	S769	S770	S771	S772	S773	S774	S775	S776	S777	S778	S779	S780	S781	S782	S783	S784	S785	S786	S787	S788	S789	S790	S791	S792	S793	S794	S795	S796	S797	S798	S799	S800	S801	S802	S803	S804	S805	S806	S807	S808	S809	S810	S811	S812	S813	S814	S815	S816	S817	S818	S819	S820	S821	S822	S823	S824	S825	S826	S827	S828	S829	S830	S831	S832	S833	S834	S835	S836	S837	S838	S839	S840	S841	S842	S843	S844	S845	S846	S847	S848	S849	S850	S851	S852	S853	S854	S855	S856	S857	S858	S859	S860	S861	S862	S863	S864	S865	S866	S867	S868	S869	S870	S871	S872	S873	S874	S875	S876	S877	S878	S879	S880	S881	S882	S883	S884	S885	S886	S887	S888	S889	S890	S891	S892	S893	S894	S895	S896	S897	S898	S899	S900	S901	S902	S903	S904	S905	S906	S907	S908	S909	S910	S911	S912	S913	S914	S915	S916	S917	S918	S919	S920	S921	S922	S923	S924	S925	S926	S927	S928	S929	S930	S931	S932	S933	S934	S935	S936	S937	S938	S939	S940	S941	S942	S943	S944	S945	S946	S947	S948	S949	S950	S951	S952	S953	S954	S955	S956	S957	S958	S959	S960	S961	S962	S963	S964	S965	S966	S967	S968	S969	S970	S971	S972	S973	S974	S975	S976	S977	S978	S979	S980	S981	S982	S983	S984	S985	S986	S987	S988	S989	S990	S991	S992	S993	S994	S995	S996	S997	S998	S999	S1000	S1001	S1002	S1003	S1004	S1005	S1006	S1007	S1008	S1009	S1010	S1011	S1012	S1013	S1014	S1015	S1016	S1017	S1018	S1019	S1020	S1021	S1022	S1023	S1024	S1025	S1026	S1027	S1028	S1029	S1030	S1031	S1032	S1033	S1034	S1035	S1036	S1037	S1038	S1039	S1040	S1041	S1042	S1043	S1044	S1045	S1046	S1047	S1048	S1049	S1050	S1051	S1052	S1053	S1054	S1055	S1056	S1057	S1058	S1059	S1060	S1061	S1062	S1063	S1064	S1065	S1066	S1067	S1068	S1069	S1070	S1071	S1072	S1073	S1074	S1075	S1076	S1077	S1078	S1079	S1080	S1081	S1082	S1083	S1084	S1085	S1086	S1087	S1088	S1089	S1090	S1091	S1092	S1093	S1094	S1095	S1096	S1097	S1098	S1099	S1100	S1101	S1102	S1103	S1104	S1105	S1106	S1107	S1108	S1109	S1110	S1111	S1112	S1113	S1114	S1115	S1116	S1117	S1118	S1119	S1120	S1121	S1122	S1123	S1124	S1125	S1126	S1127	S1128	S1129	S1130	S1131	S1132	S1133	S1134	S1135	S1136	S1137	S1138	S1139	S1140	S1141	S1142	S1143	S1144	S1145	S1146	S1147	S1148	S1149	S1150	S1151	S1152	S1153	S1154	S1155	S1156	S1157	S1158	S1159	S1160	S1161	S1162	S1163	S1164	S1165	S1166	S1167	S1168	S1169	S1170	S1171	S1172	S1173	S1174	S1175	S1176	S1177	S1178	S1179	S1180	S1181	S1182	S1183	S1184	S1185	S1186	S1187	S1188	S1189	S1190	S1191	S1192	S1193	S1194	S1195	S1196	S1197	S1198	S1199	S1200	S1201	S1202	S1203	S1204	S1205	S1206	S1207	S1208	S1209	S1210	S1211	S1212	S1213	S1214	S1215	S1216	S1217	S1218	S1219	S1220	S1221	S1222	S1223	S1224	S1225	S1226	S1227	S1228	S1229	S1230	S1231	S1232	S1233	S1234	S1235	S1236	S1237	S1238	S1239	S1240	S1241	S1242	S1243	S1244	S1245	S1246	S1247	S1248	S1249	S1250	S1251	S1252	S1253	S1254	S1255	S1256	S1257	S1258	S1259	S1260	S1261	S1262	S1263	S1264	S1265	S1266	S1267	S1268	S1269	S1270	S1271	S1272	S1273	S1274	S1275	S1276	S1277	S1278	S1279	S1280	S1281	S1282	S1283	S1284	S1285	S1286	S1287	S1288	S1289	S1290	S1291	S1292	S1293	S1294	S1295	S1296	S1297	S1298	S1299	S1300	S1301	S1302	S1303	S1304	S1305	S1306	S1307	S1308	S1309	S1310	S1311	S1312	S1313	S1314	S1315	S1316	S1317	S1318	S1319	S1320	S1321	S1322	S1323	S1324	S1325	S1326	S1327	S1328	S1329	S1330	S1331	S1332	S1333	S1334	S1335	S1336	S1337	S1338	S1339	S1340	S1341	S1342	S1343	S1344	S1345	S1346	S1347	S1348	S1349	S1350	S1351	S1352	S1353	S1354	S1355	S1356	S1357	S1358	S1359	S1360	S1361	S1362	S1363	S1364	S1365	S1366	S1367	S1368	S1369	S1370	S1371	S1372	S1373	S1374	S1375	S1376	S1377	S1378	S1379	S1380	S1381	S1382	S1383	S1384	S1385	S1386	S1387	S1388	S1389	S1390	S1391	S1392	S1393	S1394	S1395	S1396	S1397	S1398	S1399	S1400	S1401	S1402	S1403	S1404	S1405	S1406	S1407	S1408	S1409	S1410	S1411	S1412	S1413	S1414	S1415	S1416	S1417	S1418	S1419	S1420	S1421	S1422	S1423	S1424	S1425	S1426	S1427	S1428	S1429	S1430	S1431	S1432	S1433	S1434	S1435	S1436	S1437	S1438	S1439	S1440	S1441	S1442	S1443	S1444	S1445	S1446	S1447	S1448	S1449	S1450	S1451	S1452	S1453

families (Family 3/S5 and Family 4/S7) were at the lower end of the spectrum with a reduced C28/26 ratio in the patients' DBSs when compared to controls, which parallels the global VLCFA reduction (\geq C28) including ceramide/glucosylceramide and free fatty acids in homozygous *Elovl4*^{del/del} mice (Vasireddy et al., 2007). From this limited amount of measurements, the calculation of the C28:0-LysoPC over C26:0-lysoPC ratio in DBS appears to be a potential biomarker for this disorder but to confirm that this biomarker is indeed usable in clinical practice, more method development/validation should be performed and more *ELOVL4*-deficient subjects should be evaluated.

Molecular analyses in two unrelated families from same tribe showed a novel homozygous exonic deletion CNV, unlike the previously reported cases with ISQMR who had deleterious SNVs, yet leading to similar presentation (Aldahmesh et al., 2011; Diociaiuti et al., 2021; Mir et al., 2014). Evidence suggests that up to 8% of AR disorders are caused by homozygous CNVs (Yuan et al., 2020). The majority of homozygous CNVs resulting in AR conditions affect a single gene, and closer to half affect one exon as seen here (Yuan et al., 2020). Yet, small homozygous CNVs (<1000 kb) are often overlooked due to the limitation of CMA and aCGH in detecting small genetic and intragenic CNVs (<400 Kb). New bioinformatic algorithms have been proven sensitive in detecting small homozygous intragenic deletion (<50 Kb) from exome data (Duan et al., 2021; Gambin et al., 2017). Concurrent CMA and ES can optimize the diagnostic rate and allow more precise detection of small CNVs (Dharmadhikari et al., 2019). Retrospective review of CMA data in proband of Family 1 showed that the *ELOVL4* variant falls within a large run of homozygosity (ROH) and that there are six missing probes in aCGH data compared to control (Figure 3). The homozygous deletion was later confirmed by QPCR. It thus may be worth investigating such smaller CNVs detected on aCGH when it falls within an ROH interval, especially in highly consanguineous population in which the burden of AR disorders is high.

Interestingly, proband of Family 1 had cousins with a severe neurological disorder, yet; exome data proved the presence of two different molecular and neurological conditions within the same extended family (Figure 1a). Multi-locus pathogenic variation is a well-established cause for a blended phenotype in an affected individual and for intrafamilial variability such as in this extended pedigree (Karaca et al., 2018; Posey et al., 2017). This finding of two rare Mendelian AR disorders within the same extended family has implications not only on clinical diagnosis but also on counseling and family planning. Around 10% of consanguineous couples with an affected child have a second shared pathogenic or likely pathogenic variant leading to a second AR disease of moderate to profound

severity (Mor-Shaked et al., 2021). Both parents in Family 1 were confirmed heterozygous carriers of *ELOVL4* variant, and testing for the *TBCK* variant was also strongly recommended in this couple undergoing preimplantation genetic diagnosis (PGD) so that both pathogenic variants are considered in planning to avoid the risk of having a child with a second, unrelated disorder.

The finding of two seemingly unrelated probands with the same *ELOVL4* variant in Families 1 and 2 from same tribe suggest that the *ELOVL4* variant is potentially a founder allele within their large tribe. Testing similarly affected individuals from the Middle East region for this exonic deletion is advisable.

In conclusion, we report four additional families harboring novel homozygous *ELOVL4* variants and ISQMR; two Saudi families from the same tribe harboring a novel homozygous exonic deletion, and two other families with novel missense variants, one from Pakistan and the other from Saudi Arabia. Our report improves the understanding of the phenotypic features of *ELOVL4*-related ISQMR, expands the genotypic spectrum of the disorder, and adds to the global effort of understanding this rare disease. The increasing clinical application of next-generation sequencing will likely lead to the identification of additional cases and allow for further delineation of the clinical and biochemical phenotype of *ELOVL4*-related ISQMR.

AUTHOR CONTRIBUTIONS

Fatima Al-abdulrazzaq and Dana Marafi contributed to drafting the manuscript and revising it critically for important intellectual content. Fatima Al-abdulrazzaq, Talal Alanzi, Dana Marafi, Ashraf H. Aboelane, Amira Abdullah, Alice Gardham, Emma Wakeling, Harry G Leitch, Moeenaldeen AlSayed, Maha Abdulrahim, Amal Alwadani, and Laila Bastaki contributed to data acquisition, including clinical examination of patients, clinical images, sample collection, and genetic counseling. Haya H Al-Balool, Abdulaziz Aladwani, Antonio Romito, and Kapil Kampe performed the QPCR and breakpoint experiments and analyzed patient data and drafted the genetic reports. Frédéric M Vaz and Sasha Ferdinandusse performed and interpreted the biochemical analysis of VLCFA-containing LysoPCs. Aida Bertoli-Avella and Dana Marafi contributed to the analysis and interpretation of the data and critical review of the manuscript. All authors approved the final manuscript and agreed to be accountable for all aspects of the work.

ACKNOWLEDGMENTS

We would like to thank the families for their participation in this study and Henk van Lenthe for expert technical

assistance for the measurement of VCLFA-containing lysophosphatidylcholines.

FUNDING INFORMATION

This research received no external funding.

CONFLICT OF INTEREST STATEMENT

AR, KK, and AMBA are employees of CENTOGENE GmbH. Other authors have no potential conflicts to report.

DATA AVAILABILITY STATEMENT

All data included in this manuscript are available and can be de-identified and shared upon request to corresponding author.

ORCID

Fatima Alabdulrazzaq  <https://orcid.org/0009-0003-0052-8163>

Alice Gardham  <https://orcid.org/0000-0002-6556-366X>

Frédéric M. Vaz  <https://orcid.org/0000-0002-9048-1041>

Aida M. Bertoli-Avella  <https://orcid.org/0000-0001-9544-1877>

Dana Marafi  <https://orcid.org/0000-0003-2233-3423>

REFERENCES

- Agbaga, M. P. (2016). Different mutations in *ELOVL4* affect very long chain fatty acid biosynthesis to cause variable neurological disorders in humans. *Advances in Experimental Medicine and Biology*, 854, 129–135. https://doi.org/10.1007/978-3-319-17121-0_18
- Agbaga, M. P., Brush, R. S., Mandal, M. N., Henry, K., Elliott, M. H., & Anderson, R. E. (2008). Role of Stargardt-3 macular dystrophy protein (*ELOVL4*) in the biosynthesis of very long chain fatty acids. *Proceedings of the National Academy of Sciences of the United States of America*, 105(35), 12843–12848. <https://doi.org/10.1073/pnas.0802607105>
- Agbaga, M. P., Mandal, M. N., & Anderson, R. E. (2010). Retinal very long-chain PUFAs: New insights from studies on *ELOVL4* protein. *Journal of Lipid Research*, 51(7), 1624–1642. <https://doi.org/10.1194/jlr.R005025>
- Aldahmesh, M. A., Mohamed, J. Y., Alkuraya, H. S., Verma, I. C., Puri, R. D., Alaiya, A. A., Rizzo, W. B., & Alkuraya, F. S. (2011). Recessive mutations in *ELOVL4* cause ichthyosis, intellectual disability, and spastic quadriplegia. *American Journal of Human Genetics*, 89(6), 745–750. <https://doi.org/10.1016/j.ajhg.2011.10.011>
- Beaudoin, F., Wu, X., Li, F., Haslam, R. P., Markham, J. E., Zheng, H., Napier, J. A., & Kunst, L. (2009). Functional characterization of the Arabidopsis beta-ketoacyl-coenzyme A reductase candidates of the fatty acid elongase. *Plant Physiology*, 150(3), 1174–1191. <https://doi.org/10.1104/pp.109.137497>
- Bourassa, C. V., Raskin, S., Serafini, S., Teive, H. A., Dion, P. A., & Rouleau, G. A. (2015). A new *ELOVL4* mutation in a case of spinocerebellar ataxia with Erythrokeratoderma. *JAMA Neurology*, 72(8), 942–943. <https://doi.org/10.1001/jaman.2015.0888>
- Deák, F., Anderson, R. E., Fessler, J. L., & Sherry, D. M. (2019). Novel cellular functions of very long chain-fatty acids: Insight from *ELOVL4* mutations. *Frontiers in Cellular Neuroscience*, 13, 428. <https://doi.org/10.3389/fncel.2019.00428>
- Dharmadhikari, A. V., Ghosh, R., Yuan, B., Liu, P., Dai, H., al Masri, S., Scull, J., Posey, J. E., Jiang, A. H., He, W., Vetrini, F., Braxton, A. A., Ward, P., Chiang, T., Qu, C., Gu, S., Shaw, C. A., Smith, J. L., Lalani, S., ... Bi, W. (2019). Copy number variant and runs of homozygosity detection by microarrays enabled more precise molecular diagnoses in 11,020 clinical exome cases. *Genome Medicine*, 11(1), 30. <https://doi.org/10.1186/s13073-019-0639-5>
- Diociaiuti, A., Martinelli, D., Nicita, F., Cesario, C., Pisaneschi, E., Macchiaiolo, M., Rossi, S., Condorelli, A. G., Zambruno, G., & el Hachem, M. (2021). Two Italian patients with *ELOVL4*-related neuro-ichthyosis: Expanding the genotypic and phenotypic spectrum and ultrastructural characterization. *Genes (Basel)*, 12(3), 343. <https://doi.org/10.3390/genes12030343>
- Duan, R., Saadi, N. W., Grochowski, C. M., Bhadila, G., Faridoun, A., Mitani, T., du, H., Fatih, J. M., Jhangiani, S. N., Akdemir, Z. C., Gibbs, R. A., Pehlivan, D., Posey, J. E., Marafi, D., & Lupski, J. R. (2021). A novel homozygous *SLC13A5* whole-gene deletion generated by *Alu/Alu*-mediated rearrangement in an Iraqi family with epileptic encephalopathy. *American Journal of Medical Genetics. Part A*, 185(7), 1972–1980. <https://doi.org/10.1002/ajmg.a.62192>
- Fischer, J., & Bourrat, E. (2020). Genetics of inherited ichthyoses and related diseases. *Acta Dermato-Venereologica*, 100(7), adv00096. <https://doi.org/10.2340/00015555-3432>
- Gambin, T., Akdemir, Z. C., Yuan, B., Gu, S., Chiang, T., Carvalho, C. M. B., Shaw, C., Jhangiani, S., Boone, P. M., Eldomery, M. K., Karaca, E., Bayram, Y., Stray-Pedersen, A., Muzny, D., Charng, W. L., Bahrambeigi, V., Belmont, J. W., Boerwinkle, E., Beaudet, A. L., ... Lupski, J. R. (2017). Homozygous and hemizygous CNV detection from exome sequencing data in a Mendelian disease cohort. *Nucleic Acids Research*, 45(4), 1633–1648. <https://doi.org/10.1093/nar/gkw1237>
- Hopiavuori, B. R., Deák, F., Wilkerson, J. L., Brush, R. S., Rocha-Hopiavuori, N. A., Hopiavuori, A. R., Ozan, K. G., Sullivan, M. T., Wren, J. D., Georgescu, C., Szweda, L., Awasthi, V., Towner, R., Sherry, D. M., Anderson, R. E., & Agbaga, M. P. (2018). Homozygous expression of mutant *ELOVL4* leads to seizures and death in a novel animal model of very long-chain fatty acid deficiency. *Molecular Neurobiology*, 55(2), 1795–1813. <https://doi.org/10.1007/s12035-017-0824-8>
- Jaspers, Y. R. J., Ferdinandusse, S., Dijkstra, I. M. E., Barendsen, R. W., van Lenthe, H., Kulik, W., Engelen, M., Goorden, S. M. I., Vaz, F. M., & Kemp, S. (2020). Comparison of the diagnostic performance of C26:0-Lysophosphatidylcholine and very long-chain fatty acids analysis for peroxisomal disorders. *Frontiers in Cell and Developmental Biology*, 8, 690. <https://doi.org/10.3389/fcell.2020.00690>
- Karaca, E., Posey, J. E., Coban Akdemir, Z., Pehlivan, D., Harel, T., Jhangiani, S. N., Bayram, Y., Song, X., Bahrambeigi, V., Yuregir, O. O., Bozdogan, S., Yesil, G., Isikay, S., Muzny, D., Gibbs, R. A., & Lupski, J. R. (2018). Phenotypic expansion illuminates multilocus pathogenic variation. *Genetics in Medicine*, 20(12), 1528–1537. <https://doi.org/10.1038/gim.2018.33>
- Leonard, A. E., Pereira, S. L., Sprecher, H., & Huang, Y. S. (2004). Elongation of long-chain fatty acids. *Progress in Lipid Research*, 43(1), 36–54. [https://doi.org/10.1016/s0163-7827\(03\)00040-7](https://doi.org/10.1016/s0163-7827(03)00040-7)

- McDonald-McGinn, D. M., Sullivan, K. E., Marino, B., Philip, N., Swillen, A., Vorstman, J. A., Zackai, E. H., Emanuel, B. S., Vermeesch, J. R., Morrow, B. E., Scambler, P. J., & Bassett, A. S. (2015). 22q11.2 deletion syndrome. *Nature Reviews. Disease Primers*, 1, 15071. <https://doi.org/10.1038/nrdp.2015.71>
- Mir, H., Raza, S. I., Touseef, M., Memon, M. M., Khan, M. N., Jaffar, S., & Ahmad, W. (2014). A novel recessive mutation in the gene *ELOVL4* causes a neuro-ichthyotic disorder with variable expressivity. *BMC Medical Genetics*, 15, 25. <https://doi.org/10.1186/1471-2350-15-25>
- Monies, D., Abouelhoda, M., AlSayed, M., Alhassnan, Z., Alotaibi, M., Kayyali, H., al-Owain, M., Shah, A., Rahbeeni, Z., al-Muhaizea, M. A., Alzaidan, H. I., Cupler, E., Bohlega, S., Faqeih, E., Faden, M., Alyounes, B., Jaroudi, D., Goljan, E., Elbardisy, H., ... Alkuraya, F. S. (2017). The landscape of genetic diseases in Saudi Arabia based on the first 1000 diagnostic panels and exomes. *Human Genetics*, 136(8), 921–939. <https://doi.org/10.1007/s00439-017-1821-8>
- Mor-Shaked, H., Rips, J., Gershon Naamat, S., Reich, A., Elpeleg, O., Meiner, V., & Harel, T. (2021). Parental exome analysis identifies shared carrier status for a second recessive disorder in couples with an affected child. *European Journal of Human Genetics*, 29(3), 455–462. <https://doi.org/10.1038/s41431-020-00756-y>
- Posey, J. E., Harel, T., Liu, P., Rosenfeld, J. A., James, R. A., Coban Akdemir, Z. H., Walkiewicz, M., Bi, W., Xiao, R., Ding, Y., Xia, F., Beaudet, A. L., Muzny, D. M., Gibbs, R. A., Boerwinkle, E., Eng, C. M., Sutton, V. R., Shaw, C. A., Plon, S. E., ... Lupski, J. R. (2017). Resolution of disease phenotypes resulting from multi-locus genomic variation. *The New England Journal of Medicine*, 376(1), 21–31. <https://doi.org/10.1056/NEJMoa1516767>
- Rizzo, W. B., Jenkins, S. M., & Boucher, P. (2012). Recognition and diagnosis of neuro-ichthyotic syndromes. *Seminars in Neurology*, 32(1), 75–84. <https://doi.org/10.1055/s-0032-1306390>
- Schneiter, R., Brügger, B., Amann, C. M., Prestwich, G. D., Epanand, R. F., Zellnig, G., Wieland, F. T., & Epanand, R. M. (2004). Identification and biophysical characterization of a very-long-chain-fatty-acid-substituted phosphatidylinositol in yeast subcellular membranes. *The Biochemical Journal*, 381(Pt 3), 941–949. <https://doi.org/10.1042/bj20040320>
- Sullivan, R., Yau, W. Y., O'Connor, E., & Houlden, H. (2019). Spinocerebellar ataxia: an update. *Journal of Neurology*, 266(2), 533–544. <https://doi.org/10.1007/s00415-018-9076-4>
- Tvrđik, P., Westerberg, R., Silve, S., Asadi, A., Jakobsson, A., Cannon, B., Loison, G., & Jakobsson, A. (2000). Role of a new mammalian gene family in the biosynthesis of very long chain fatty acids and sphingolipids. *The Journal of Cell Biology*, 149(3), 707–718. <https://doi.org/10.1083/jcb.149.3.707>
- Vasireddy, V., Uchida, Y., Salem, N., Jr., Kim, S. Y., Mandal, M. N., Reddy, G. B., Bodepudi, R., Alderson, N. L., Brown, J. C., Hama, H., Dlugosz, A., Elias, P. M., Holleran, W. M., & Ayyagari, R. (2007). Loss of functional *ELOVL4* depletes very long-chain fatty acids (> or =C28) and the unique omega-O-acylceramides in skin leading to neonatal death. *Human Molecular Genetics*, 16(5), 471–482. <https://doi.org/10.1093/hmg/ddl480>
- Yuan, B., Wang, L., Liu, P., Shaw, C., Dai, H., Cooper, L., Zhu, W., Anderson, S. A., Meng, L., Wang, X., Wang, Y., Xia, F., Xiao, R., Braxton, A., Peacock, S., Schmitt, E., Ward, P. A., Vetrini, F., He, W., ... Bi, W. (2020). CNVs cause autosomal recessive genetic diseases with or without involvement of SNV/indels. *Genetics in Medicine*, 22, 1633–1641. <https://doi.org/10.1038/s41436-020-0864-8>

How to cite this article: Alabdulrazzaq, F., Alanzi, T., Al-Balool, H. H., Gardham, A., Wakeling, E., Leitch, H. G., AlSayed, M., Abdulrahim, M., Aladwani, A., Romito, A., Kampe, K., Ferdinandusse, S., Aboelanine, A. H., Abdullah, A., Alwadani, A., Bastaki, L., Vaz, F. M., Bertoli-Avella, A. M., & Marafi, D. (2023). Expanding the allelic spectrum of *ELOVL4*-related autosomal recessive neuro-ichthyosis. *Molecular Genetics & Genomic Medicine*, 00, e2256. <https://doi.org/10.1002/mgg3.2256>